

208400099

CENTRAL INSTITUTE OF PHYSICS
INSTITUTE FOR PHYSICS AND NUCLEAR ENGINEERING
Bucharest, POB MG-6, ROMANIA

JINR-DUBNA, USSR^{*)}

ISTITUTO DI FISICA DELL'UNIVERSITA - TORINO, ITALY^{**)}

IFIN - HE-101-1981

June

Energy dependence phase shift analysis of
 ^3He elastic scattering and the possibility
of the (^3He) excited states existence

F. Nichitiu, I.V. Falomkin^{*)}, M.G. Sapozhnikov^{*)}
Yu.A. Shcherbakov^{*)}, G. Piragino^{**)}

Abstract

In the 24 MeV - 260 MeV kinetic energy interval, the energy dependent phase shift analysis of ^3He elastic scattering is done. The energy dependence is given by the rational fraction approximants of the partial S matrix. The search for the stable S matrix zero-pole pairs in the k and \sqrt{s} complex plane give some proofs for the existence of the (^3He) excited states in the S, P and probably D partial waves.

1. Introduction

As usual, the aim of the phase shift analysis is twofold. The first goal is to determine the scattering amplitude as a complex function of two variables (energy and scattering angle) in order to have a convenient parametrization of the experimental data and to test some theoretical models. The second goal is to analyse the scattering amplitude in order to determine the resonance spectrum, that is, to find from the energy dependence of the partial wave amplitude the mass and the width of the resonances. This last purpose of the phase shift analysis is used for scattering of elementary particles like πN , $\bar{N} N$ or $K N$.

As usual, the experimental data of particle-nucleus scattering are described by models without partial wave analysis. Anyway, in the last time, some phase shift analysis, specially for pion-nucleus scattering was done [1-9,14]. The purposes of these analyses were electromagnetic pion radius determination [10,11], for the use of partial wave in nuclear α cluster models [12], optical model test at the partial wave level [7] or even the search for resonant behaviour of the partial wave. This last problem (the existence of the multiparticle resonance of the pion-nucleus system in the region of the first baryon resonance Δ_{33}) is now debated in literature [15-19] but mainly from the nuclear models point of view and so, the existence or non-existence of such kind of multibarionic resonance is inconclusive.

If the resonance has a sufficient small width, a signal of its existence can be obtained easily from the energy dependence of the total cross section.

For pion-nucleus scattering there is wide maximum in total cross section around 150 MeV kinetic energy and the supposed resonance (or resonances) of this system cannot be proved without

a detailed phase shift analysis.

The first indications concerning the possible existence of the ${}^4\text{He}$ resonances are given in /3,13/ where a resonance behaviour in the energy dependence of the P and D partial wave has been shown.

In this paper we present an energy dependence phase shift analysis of ${}^4\text{He}$ elastic scattering using for partial S matrix parametrization a rational fraction approximant.

Due to complications rised by resonance to background addition and by the widths energy dependence, we consider as the best criterium for resonance determination, the existence near the physical region of a S matrix zero-pole pair in the complex momentum or energy plane /20,21/. This criterium is of course a correct one as correct is phase shift analysis itself. The criterium was tested by using the Padé approximant of type II and III to the partial S matrix of pion-nucleon interaction /22/.

II. Description of the method

The differential cross section for ${}^4\text{He}$ elastic scattering is given by:

$$\frac{d\sigma}{d\Omega} = |f_c + f_{cN}|^2 \quad (1)$$

where $f_{cN}(x,k) = \frac{1}{k} \sum (2l+1) e^{2i\tau_l} r_l(k) P_l(x)$

is the scattering amplitude at $x = \cos \theta$ and cM-momentum k . The f_c and τ_l are coulomb scattering amplitude and coulomb phase shift, and $r_l(k)$ is the partial wave amplitude.

Real part of the forward scattering amplitude and the total cross section are given by nuclear amplitude:

$$f_N(x,k) = \frac{1}{k} \sum (2l+1) r_l(k) P_l(x) \quad (2)$$

In our energy dependence phase shift analysis we have used for the energy parametrisation of the partial S matrix:

$$S_l(k) = 1 + 2if_l(k)$$

a factorization procedure:

$$S_l(k) = S_l^{(I)}(k) \cdot S_l^{(II)}(k) \quad (3)$$

The first factor in eq. (3) has its main contribution in the low energy region and the second one give the contribution at medium and asymptotic energy region.

It is well known that a good approximant for a complex analytic function, as the partial S matrix, can be achieved by diagonal Padé approximants where the zero and poles can have physical meanings /22,26/. In ours, we choose a ratio of two polynomials for the second factor in eq. (3). The power of both polynomials from the S matrix rational fraction will depend on the orbital momentum l . Near the elastic threshold, the S matrix energy dependence is given by:

$$S_l^{(I)}(k) = \frac{1 - 2ia_l k^{2l+1}}{1 + 2ia_l k^{2l+1}} \quad (4)$$

due to the effective range behaviour of the partial wave

$$k^{2l+1} \operatorname{ctg} \sigma_l \xrightarrow[k \rightarrow 0]{} -1/2 \cdot a_l, \quad (5)$$

where $2a_l$ is the complex scattering length.

For very low energy we need for the partial S matrix energy dependence a limit similar to (5):

$$S_l(k) \xrightarrow[k \rightarrow 0]{} S_l^{(I)}(k) \xrightarrow[k \rightarrow 0]{} 1 \quad (6)$$

Due to the fact that at very low energy, the second factor from eq. (3) must tend to unity more rapidly than the first one:

$$S_l^{(II)}(k) \xrightarrow[k \rightarrow 0]{} 1 \text{ faster than eq. (6)}$$

the lowest power of k in $S_1^{(II)}(k)$ should be larger than $2l+1$

On the other hand, for $k \rightarrow \infty$ the S matrix must be unitary

$$S_1(k) \xrightarrow[k \rightarrow \infty]{} \beta_{\infty} e^{2i\delta_{\infty}} \quad \text{with } 0 \leq \eta_{\infty} \leq 1 \quad (7)$$

Therefore, the larger power of k in $S_1^{(II)}(k)$ should have the coefficient $\exp 2ia_5$ where a_5 is a complex parameter with $\text{Im}a_5 \geq 0$.

For the second factor of eq. (3) we use the following parametrization:

$$S_1^{(II)}(k) = \frac{1 + a_2 k^{2l+2} + a_5 e^{2ia_5} (1 + 2ia_1 k^{2l+1}) k^{2l+N}}{1 + a_2 k^{2l+2} + a_5 (1 - 2ia_1 k^{2l+1}) k^{2l+N}} \quad (8)$$

where $N = 3$ or 4 .

With this form of $S_1^{(II)}(k)$ we can obtain for very large k the eq. (7) because:

$$S_1^{(II)}(k) \xrightarrow[k \rightarrow \infty]{} \left[S_1^{(I)}(k) \right]^{-1} e^{2ia_5}$$

The partial S matrix is factorized form (eq. 3) with $S_1^{(I)}(k)$ and $S_1^{(II)}(k)$ given by eq. (4) and eq. (8) respectively, has correct energy behaviour near the threshold and at large energy and represent a rational fraction approximant.

The maximum number of the partial waves taken into account in our analysis is $L = 4$ and each partial wave is represented by 5 complex constants a_1, \dots, a_5 .

The solutions obtained with $N = 4$ and 3 in eq. (8) are called S_A and S_B respectively.

In order to test the influence of the high partial wave especially for the analysis of zero-pole pair stability in k complex plane, we have approximated the S wave by the effective range

behaviour, that is only $S_a^{(I)}(k)$ and all other waves with eq.(3) for $N = 3$ in eq. 8 (solution S_c).

III. The analysis of the experimental data

The experimental data used in our energy dependence phase shift analysis consists in 11 differential cross sections of ^4He elastic scattering in the energy interval from 24 MeV to 260 MeV [1,2,7,8] (310 data points), 21 data on the total cross section (from 51 MeV to 273 MeV) [8,23-25] and 7 values for the real part of the forward scattering amplitude (25 MeV - 200 MeV) from the standard dispersion relations calculations. The errors used for Ref(0) are larger than the error corridor given by dispersion relations calculations.

For the total number of experimental data $N_p = 338$, the maximal number of parameters is $N_{\text{par}} = 50$. Due to the very small value and large error of some parameters, the actual number of the free parameters used is less than 50. Some features of our fit with all three variants are presented in table I.

The large values of the χ^2 are due to incompatibility of the different sets of the experimental data. In our energy dependent phase shift analysis we have not used any normalization errors.

Figure 1 shows the energy dependence of the total and elastic cross section given by each parametrization used in our phase shift analysis. The fit of the experimental data is good. The elastic cross section data are from ref. [8] and are not used in fitting procedure. In the low energy region, the total cross section has an energy dependence like $1/v$, which is typical for reactions with absorption at the threshold.

A broad maximum is seen in both cross sections of $T = 150$ MeV

for total cross section and at $T = 180$ Mev for elastic cross section.

The real part of the forward amplitude is in good agreement with the experimental data of Ref(0) obtained from the coulomb interference analysis in ref. [8] (these data are not included in our fitting procedure) (fig. 2). We remark that the noticed in ref. [27] discrepancy between experimental data of Ref(0) at $T = 260$ Mev and dispersion relations calculation disappears in our phase shift analysis. This agreement happens probably because of our different extrapolation procedure below the threshold. The $\text{Re}f(0) = 0$ at the two energies, in low energy region at $T = 18$ Mev and in the "resonance" region at $T = 175$ - 180 Mev. The maximum value of $\text{Re}f(0) = 1$ fm is reached at $T = 110$ Mev.

The energy dependence of the forward differential cross section shows a maximum around $T = 200$ Mev (fig. 3). As above, the experimental points from ref. [8] are not taken in our fit. In all three figures, one can observe for S_B and S_C parametrisation an unsmooth behaviour around $T = 80$ Mev. It is caused by the existence in the partial S matrix of a zero and a pole localized in practically the same position in the complex k plane. Such zero-pole pairs appear in the P and D partial waves very close to the physical region (at $k = 140$ Mev and $k = 155$ Mev respectively - fig. 11b and c). This unusual behaviour which is not reflecting a real physical phenomenon, but rather the bad statistics of experimental information - is also presented in fig. 4 (only S_B parametrization). Due to the large errors in this energy region we can conclude that a smooth behaviour through the error corridor is anyway more acceptable. The energy dependence of the nuclear differential cross section

at $\theta = 180^\circ$ shows similar behaviour in all three parametrizations; there is a maximum in the region of $T = 50-80$ Mev and a minimum for $T = 160$ Mev (fig. 5). The S partial wave shows a smooth behaviour in energy and close by for all three parametrizations (fig. 6), in good agreement with the other determinations [6,7,8]. At low energies, there is a very small maximum in $\text{Im}f_0$ (at $T = 18$ Mev) (more evident in S_A parametrization). This maximum is probably connected with the influence of the excited states of the ^4He , effect observed in ref. [7]. The Argand diagrams of the partial wave amplitude obtained in our energy dependent phase shift analysis are presented in fig. 7. The general trend is similar in all three parametrizations. The "classical" resonant behaviour is evident in $l = 1$ and $l = 2$ partial wave. The S partial wave has $\text{Re}f_0 < 0$ for the whole energetical interval having an anticlockwise trajectory in Argand diagram above 150 Mev. The possible S wave resonance can be only in the presence of a strong repulsive background (for $T = 160-170$ Mev).

IV. Ambiguity analysis

In practical phase shift analysis it is assumed that the scattering amplitude (eq. 2) is well approximated by a finite sum of Legendre polynomials. The sum up to a fixed L (eq. 2) is a polynomial of degree L and so it can be written as a product of zeros terms [28]:

$$f_N(x,k) = f(1,k) \prod_{i=1}^L \frac{x-x_i(k)}{1-x_i(k)} = f(0,k) \prod_{k=1}^L \frac{t_i(k)-t}{t_i(k)} \quad (9)$$

$$t = 2k^2(1-x)$$

where $x_i(k)$ or $t_i(k)$ are the complex roots of the scattering

amplitude in the complex $\cos \theta$ or t plane. From eq. (9) it is easy to see that the differential and total cross section ($|f(x,k)|^2$ and $\text{Im}f(0,k)$) are invariant under the transformations

$$x_i(k) \leftrightarrow x_i^*(k) \quad (10)$$

for all combinations of index i . Such a transformation results in changing in 2^L possibilities for the scattering amplitude. With reversed sign of $\text{Re}f(1,k)$ we obtain 2^{L+1} solutions, but the sign of the real part of scattering amplitude is fixed by Coulomb interference and/or dispersion relations calculations.

The 2^L scattering amplitudes obtained by the transformation (10) are not all physically acceptable. By partial wave projection, we can convert the scattering amplitude (9) with the transformation (10) into partial wave expansion eq. 2 and exclude the ununitary solutions. As usual, the real number of ambiguity solutions N_a is less than the maximum number 2^L and is increasing with energy.

At a very low energy, the number of equivalent amplitudes is small and so the zero-complex-conjugation ambiguity is practically absent. This fact, together with the hypothesis of smooth zero trajectory $x_i(k)$ or $t_i(k)$, give a real possibility of finding a unique solution by inspection of the continuity of the trajectory.

The $t_i(k)$ trajectory of the scattering amplitude (eq.9) obtained in our energy dependent phase shift analysis are presented in fig. 8. For S_A and S_B parametrization of the partial wave S matrix there are 4 trajectories of zeros. For S_C parametrization, due to the very low weight of the G wave, the 4-th zero trajectory is very far from the physical region. The

zero trajectory noted by 1 is very similar for all three analyses. This zero is connected with the existence of the first deep minimum in the differential cross section. At low energies, the trajectory nr. 3 and 4 have almost complex conjugate position in complex t plane (for S_A and S_B) due to the small weight of the high partial waves.

From this analysis of the zero trajectory continuity in complex t plane, we can conclude that solutions presented in fig. 7 are unique, from the point of view of ambiguity given by transformations (10) and we must accept them as different approximations of the same physical solution.

V. Excited states of ($\pi^4\text{He}$) system

The resonant behaviour of the partial wave amplitudes can be easily observed in Argard's diagrams (fig. 7).

When a resonance is present in a partial wave but without a perturbative background, the real part of the partial wave amplitude must go to zero at the resonant energy. This is a classical test for resonance. For our P wave amplitude $\text{Re} f_1(k) = 0$ for $T = 165-210$ Mev (fig. 9) which means a large sensitivity to the parametrization used.

As usual, the definition of the resonance is given by the zero-pole pair of the partial S matrix in the k or \sqrt{s} energy plane. The physical interesting poles and zeros are those which are near the physical region. In this paper we have been searching the existence or inexistence of the ($\pi^4\text{He}$) excited states ($\pi^4\text{He}$ resonances) by analysis of the partial S matrix zero-pole pairs in the complex k (or \sqrt{s}) plane. This method is more powerful than the classical summation of a Breit-Wigner form to the energy dependent background.

The partial S matrix zeros and poles in the k (and \sqrt{s}) complex plane were determined by searching the zeros (we have used the method of Iarratt and Nudds /30/) of the numerator and of the denominator for each $S_{\mathbf{1}}^{(I)}$ and $S_{\mathbf{1}}^{(II)}$ factor from eq. 3. The positions in complex k plane of the zeros and poles of the partial S_A matrix are shown in fig. 10. In fig. 10a, very near the physical region there is a zero-pole pair which can suggest for S partial wave a resonance with elasticity $x = \frac{\Gamma_{el}}{\Gamma_{tot}} < 0.5$ at the momentum $k_A = 264$ Mev (or $\sqrt{s}_A = 4035$ Mev). The parametrizations S_B and S_C give for this zero-pole pair the values $k_B = 250$ Mev and $k_C = 254$ Mev ($\sqrt{s}_B = 4022$ Mev and $\sqrt{s}_C = 4026$ Mev). The same signal of a $\mathbf{1} = 0$ resonance with $x < 0.5$ is obtained by a similar zero-pole analysis of the S matrix but in \sqrt{s} complex plane. The values of the resonant zero-pole pair in k and \sqrt{s} complex plane are presented in table II. In order to check the existence of this resonant $\mathbf{1} = 0$ state we have tested the stability of zero-pole pairs of the S matrix using the following second order Padé approximants (P.A. II): $[3/2]$, $[3/3]$, $[4/3]$, $[4/4]$, $[5/4]$. From this analysis we have obtained the same values for the resonance parameters as from the direct search in \sqrt{s} variable of the S_C matrix. The average resonance parameters of (^4He) excited state in S wave are:

$$\sqrt{s}_p = (4028 \pm 8) - i(60 \pm 6) \text{ Mev}$$

$$\sqrt{s}_r = (4028 \pm 5) - i(24 \pm 3) \text{ Mev}$$

The mass, total and elastic width and the elasticity are:

$$M_s = 4028 \text{ Mev}$$

$$\Gamma_{tot} = 120 \text{ Mev}$$

$$\Gamma_{c2} = 36 \text{ Mev}$$

$$x = 0.3$$

The resonance zero-pole pair in complex k plane and which can be associated with the P wave resonance of the ($\pi^0\text{He}$) system (fig. 10.b and fig. 11.b) is around $k_p = 200 \text{ Mev}$ (or equivalent $\sqrt{s} = 3976 \text{ Mev}$). The values of the resonance zero-pole pairs in complex k plane are presented in table III. Here we must remark that the pole position in complex k plane is less dependent on the parametrization used than the energy value when $\text{Re} f_{\rho=; } = 0$. Due to the high k power in the polinomials of our parametrization (eq. 6 and 8) for $l = 1$ and 2 , the direct search of the zeros in \sqrt{s} complex plane fails. For these reasons the values of zero-pole pairs in \sqrt{s} complex plane was determined by P.A. II analysis. From $[4/4]$ P.A. II of S_c parametrization we have obtained the following values for the resonant zero-pole pair:

$$\sqrt{s}_p = 3959.7 - i 94.8 \text{ Mev}$$

$$\sqrt{s}_z = 4065.6 - i 0.23 \text{ Mev}$$

Using the partial wave data from ref. /8 / we have also search resonance in P wave by using the third type of Padé approximant /22/ (P.A. III is the P.A. II extension to χ^2 minimization). The $[4/4]$ P.A. III analysis in both k and \sqrt{s} complex plane give the following results:

$$k_p = 210.7 - i 75.2 \text{ Mev} \quad \sqrt{s}_p = 3970.3 - i 88.0 \text{ Mev}$$

$$k_z = 261.3 - i 21.1 \text{ Mev} \quad \sqrt{s}_z = 4041.6 - i 15.0 \text{ Mev}$$

Unfortunately, because of strong repulsive background and small

number of experimental data, this kind (P.A. III) of analysis is inconclusive for the S partial wave.

From all above tests for the P wave (^4He) resonance we can conclude that such state can probably exist having the following average parameters:

$$\sqrt{s_p} = (3965 \pm 8) - i(90 \pm 8) \text{ Mev}$$

$$\sqrt{s_z} = (4050 \pm 10) - i(8 \pm 8) \text{ Mev}$$

which means:

$$M_p = 3965 \text{ Mev}$$

$$\Gamma_{\text{tot}} = 180 \text{ Mev}$$

$$\Gamma_{\text{el}} = 90 \text{ Mev}$$

$$x = 0.5$$

For the D partial wave, the problem is more complicated. Near the real axis in the k complex plane there are two poles and only one zero (fig. 10.6). This can give rise to some ambiguous resonant interpretation.

The same aspects can be found in other parametrizations (fig. 11 for s_c).

Taken as resonant pole that one which is more close to the real axis, the k values of the resonant zero-pole pair are those presented in table IV.

The PA II in \sqrt{s} variable for S_c give for the resonance zero-pole pair the following average values

$$\sqrt{s_p} = (3984 \pm 3) - i(67 \pm 2) \text{ Mev}$$

$$\sqrt{s_z} = (4039 \pm 3) - i(37 \pm 2) \text{ Mev}$$

which means a resonance with an elasticity $x = 0.22$.

Conclusions

In this work we have presented an energy dependent phase shift analysis of ^4He elastic scattering.

For our parametrization of the energy dependence we have chosen the rational fraction approximant for the partial S matrix with a correct threshold and asymptotic behaviour. The energy behaviour of all three more important partial waves are similar to that observed in other phase shift analyses. The parametrization used gives us the possibility to undertake the analysis of the resonant structures which can exist in the partial waves by searching the zero-pole pairs of each partial S matrix in the k and \sqrt{s} complex plane.

Our phase shift and zero-pole analyses have had proof that the resonant behaviour observed in Argand diagrams can be interpreted as caused by the (^4He) excited states in S, P and probably D partial waves. This conclusion is based on the existence of the partial S matrix stable zero-pole pairs in the k and \sqrt{s} complex plane, criterium which is more powerful than the usual addition of the Breit-Wigner term to the nonresonant background. The existence of S and P resonances of the ^4He system is supported by the multiplicity of the methods in searching the stable zero-pole pairs and which give positive answer.

For $l = 1$ partial wave the P.A. III analysis of the energy independent data on partial wave support our conclusion concerning the existence of (^4He) P wave resonance too.

Table I χ^2 for S_A, S_B, S_C parametrizations

	S_A	S_B	S_C
χ^2	635	643	657
χ^2/N_P	1.88	1.90	1.94
χ^2/N_{DF}	2.14	2.21	2.20
N_{par}	42	47	40

Table II Zero-pole pairs for $l = 0$ (in k and \sqrt{s})

	in k (MeV)		in \sqrt{s} (MeV)	
	pole	zero	pole	zero
S_A	264.3 - i57.0	264.5 - i22.3	4034 - i54.6	4035.5 - i21.3
S_B	249.8 - i69.7	251.7 - i27.2	4019 - i66.0	4023.2 - i25.7
S_C	254.1 - i75.3	252.2 - i28.2	4023 - i71.1	4023.7 - i26.6

Table III Zero-pole pairs for $l = 1$ (in k)

	pole (MeV)	zero (MeV)
S_A	198.9 - i114.9	252.2 - i5.9
S_B	202.6 - i117.0	293.0 - i3.4
S_C	200.5 - i115.0	295.3 - i0.2

Table IV Zero-pole for $l = 2$ (in k)

	pole (MeV)	zero (MeV)
S_A	175. - i75.	265. - i45.
S_B	212. - i80.	275. - i42
S_C	212. - i75.	285. - i35.

R e f e r e n c e s

- /1/ M.E. Nordberg, K.F. Kinsey: *Phys. Lett.*, 20, 962 (1966)
- /2/ K. Crowe, A. Fainberg, J. Miller, A. Parsons: *Phys. Rev.*, 180, 1349 (1969)
- /3/ I.V. Falomkin, M.M. Kulyukin, V.I. Lyashenko, A. Mihul, F. Nichitiu, G. Piragino, G.B. Pontecorvo, Yu.A. Shcherbakov: Preprint JINR, E1-6534 (Dubna 1972); *Lett. Nuovo Cimento* 5, 1125 (1972)
- /4/ J. Beiner: *Nucl. Phys.* B53, 349 (1973)
- /5/ O.V. Dumbrais, F. Nichitiu, Yu.A. Shcherbakov: *Rev. Roum. Phys.* 18, 1249 (1973)
- /6/ L. Aleksandrov, T. Angelescu, I.V. Falomkin, F. Nichitiu, Yu.A. Shcherbakov: Proceeding of the International Conf. on Few-Body Problems in Nuclear and Particle Physics (Quebec, 1974) p. 348; preprint JINR P1-8328 (Dubna 1974)
- /7/ Yu.A. Shcherbakov, T. Angelescu, I.V. Falomkin, M.M. Kulyukin, V.I. Lyashenko, R. Mach, A. Mihul, N.M. Kao, F. Nichitiu, G.B. Pontecorvo, V.K. Sarycheva, M.G. Sapozhnikov, M. Semergjieva, T.M. Troshev, N.I. Trosheva, F. Balestra, L. Busso, R. Garfagnini, G. Piragino: *Nuovo Cimento*, 31A, 249 (1976)
- /8/ F. Binon, P. Duteil, M. Gouanère, L. Hugu, J. Jansen, J.P. Lagnaux, H. Palevsky, J.-P. Peigneux, M. Spighell, J.-P. Stroot: *Nucl. Phys.* A298, 499 (1978)
- /9/ I.V. Falomkin, F. Nichitiu, M.G. Sapozhnikov, Yu.A. Shcherbakov, F. Balestra, E. Bollini: *Nuovo Cimento* 43A, 604 (1978)
- /10/ F. Nichitiu, Yu.A. Shcherbakov: *Nucl. Phys.* B61, 429 (1973)
- /11/ F. Nichitiu: 5 Int. Conf. on High Energy Physics and Nuclear Structure, Uppsala, 1973, p. 178
- /12/ J.F. Germond, C. Wilkin: *Nucl. Phys.* 237A, 447 (1975)
- /13/ F. Nichitiu: Meson-Nuclear Physics, Carnegie-Mellon Conf. 1976, p. 460
- /14/ J. Arvieux, A.S. Rinat: preprint WIS-80/June-ph.

- /15/ M. Ericson, M. Krell: Phys. Lett. B38, 359 (1972)
- /16/ J. Hüfner: Phys. Rep. C21, 1 (1975)
- /17/ M. Hirata, F. Lenz, K. Yazaki: Ann. Phys. (N.Y.) 108, 116 (1977)
- /18/ K. Klingenberg, M. Dilling, M.G. Huber: Phys. Rev. Lett., 41, 387 (1978), M.G. Huber, K. Klingenberg: 11th Summer-School on Nucl. Phys. 1979; Mikolajki, Poland, p. 95
- /19/ K.W. McVoy: Nucl. Phys. A276, 491 (1977)
- /20/ K.W. McVoy: Fundamentals in Nuclear Theory, Vienna, 1967, p. 419
- /21/ F. Nichitiu: Determination of resonances by phase shift analysis, in Phys.Elec.Part.and Atom.Nuclei Moscow, 1981
- /22/ F. Nichitiu: A simple and efficient method for determination of resonance parameters by Padé approximants: Preprint IFIN, NE-99-1980
- /23/ E.C. Fowler, W.B. Fowler, R.P. Shutt, A.M. Thornidike, W.L. Whittmore: Phys. Rev. 91, 135 (1953)
- /24/ C. Wilkin, C. Cox, J. Domingo, K. Gabathuler, E. Pedroni, J. Rohlin, P. Schwaller, N. Tanner: Nucl. Phys. 62B, 61 (1973)
- /25/ K. Johnson: Thesis 1976, preprint LAMPF, LA-6561-T
- /26/ G.A. Baker Jr.: Essential of Padé approximants, Academic Press, New-York, 1975
- /27/ W. Grein, M.P. Looher: J. Phys. G: Nucl. Phys. 6, 653 (1980)
- /28/ A. Gersten: Nucl. Phys. B12, 537 (1969)
- /29/ F. Nichitiu: Lett. Nuovo Cimento 6, 547 (1973)
- /30/ P. Jarratt, D. Nudds: The Computer Journal 8, 1, (1965)

Figures captions

Fig. 1 Total and elastic cross section

————— S_A parametrization
- · - · - S_B
----- S_C

Fig. 2 Real part of the forward scattering amplitude

The curves have the same meaning as in fig. 1
The dashed area is the error corridor from the standard
dispersion relations calculations

Fig. 3 As in Fig. 1 but for the forward differential cross
section

Fig. 4 The error corridor from our phase shift analysis around
 $T \sim 80$ Mev

Fig. 5 The same as in fig 1 but for backward differential
cross section

Fig. 6 The real (a) and imaginary (b) part of the $l = 0$
partial wave amplitude. The curve notations as in fig. 1

Fig. 7 The Argand diagrams of the (a) S_A , (b) S_B and (c) S_C
parametrizations

Fig. 8 The scattering amplitude zeros trajectory in momentum
transfer t complex plane for (a) S_A , (b) S_B and (c) S_C
parametrization

Fig. 9 The real part of the $l = 1$ partial wave amplitude. The
curve notations are as in fig. 1

Fig. 10 The zeros and poles of the partial S matrix in k
plane for S_A parametrization
For (a) $l = 0$, (b) $l = 1$ and (c) $l = 1$ partial wave.
The cross \times means pole and point means zero. By arrows
are indicated the resonant zero-pole pair

Fig. 11 The same as in fig. 10 but for S_C parametrization

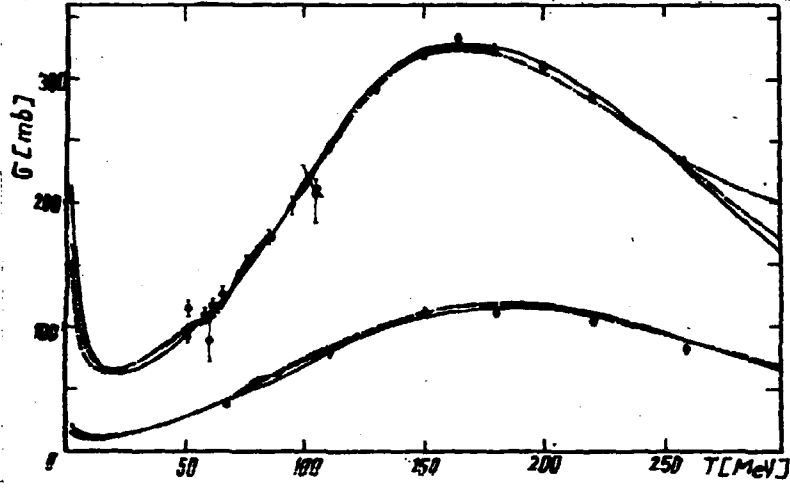


Fig.1

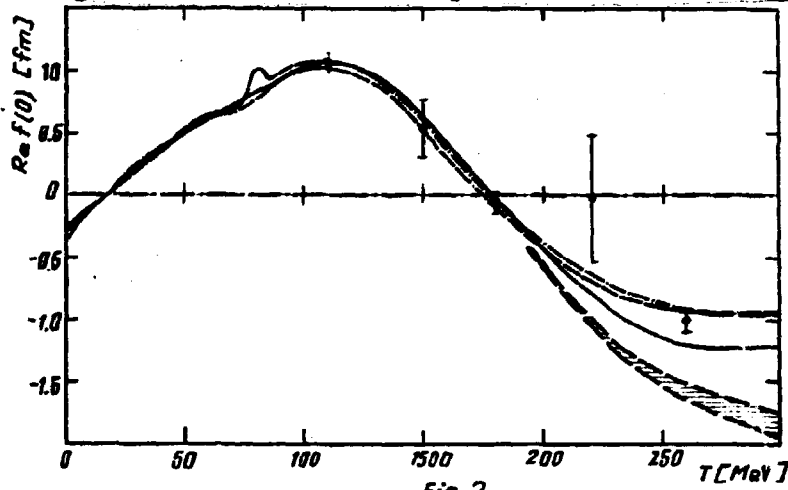


Fig.2

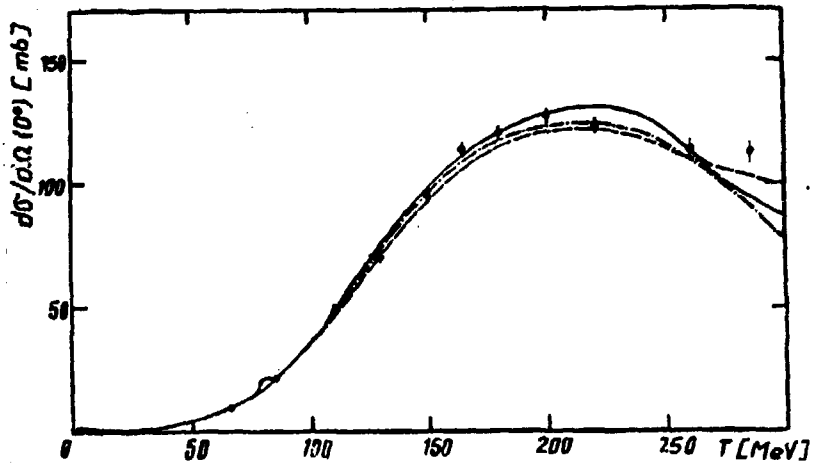


Fig.3

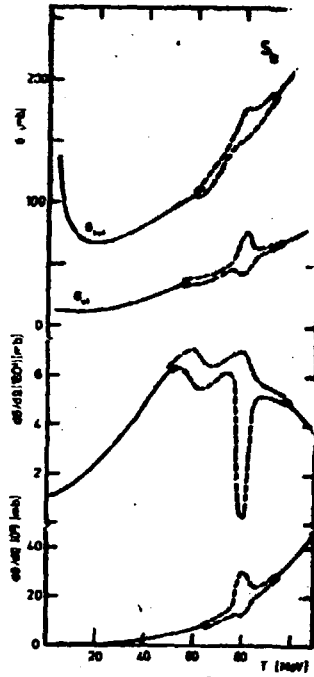


Fig. 4

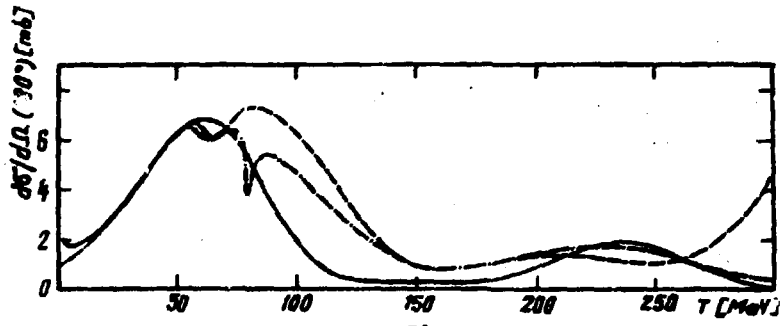


Fig. 5

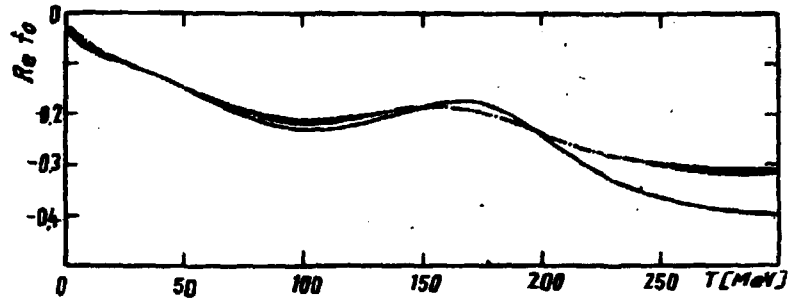


Fig. 6(a)

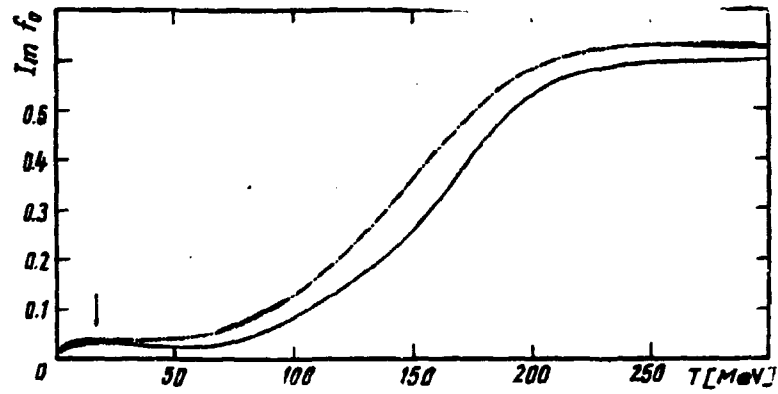


Fig. 6(b)

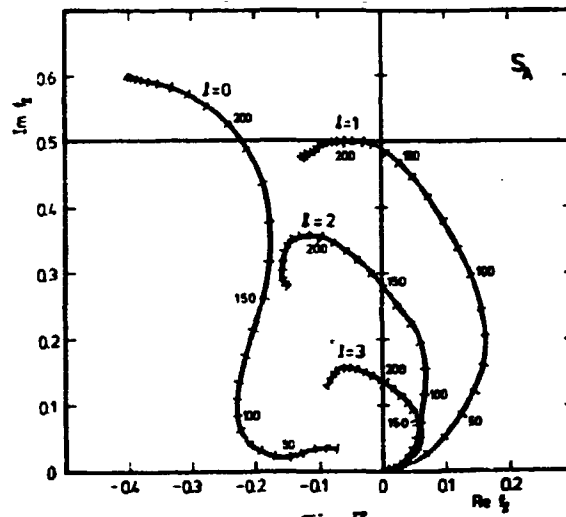


Fig. 7 a

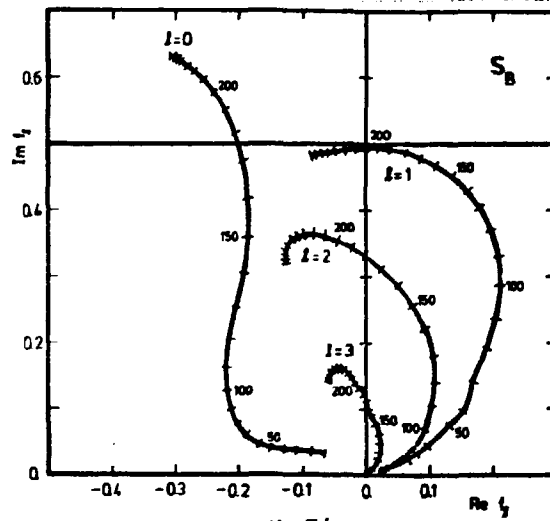


Fig. 7 b

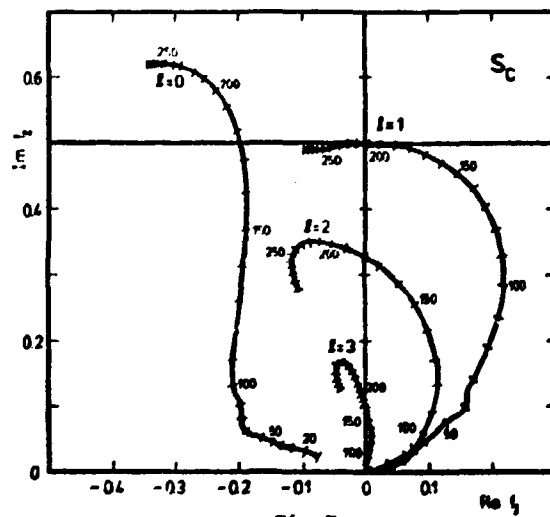


Fig. 7 c

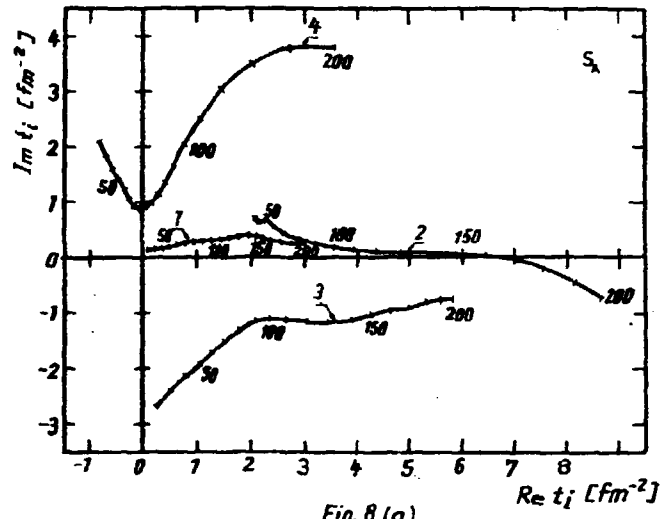


Fig. 8 (a)

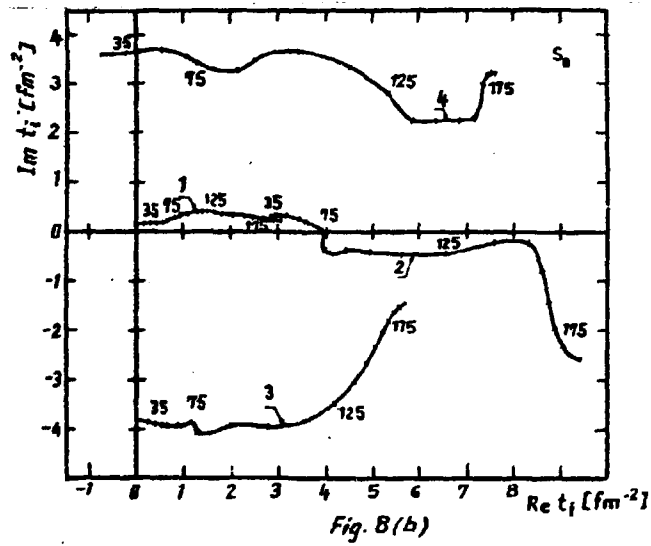


Fig. 8 (b)

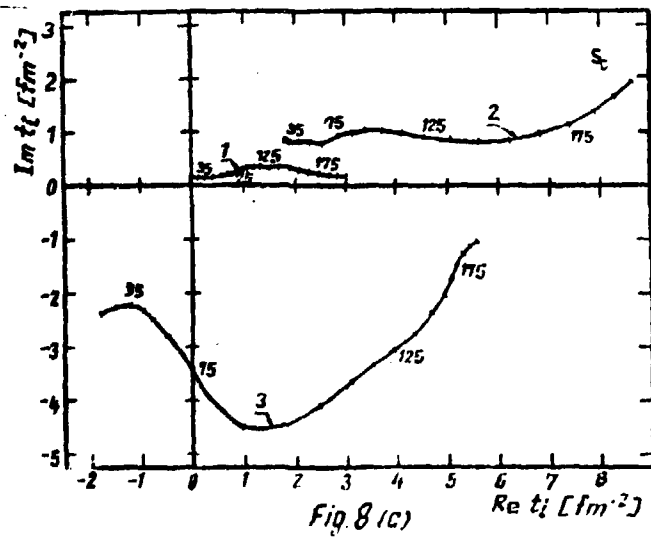


Fig. 8 (c)

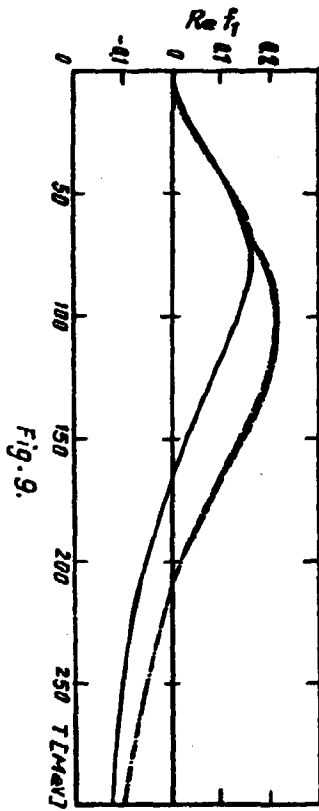


Fig. 9.

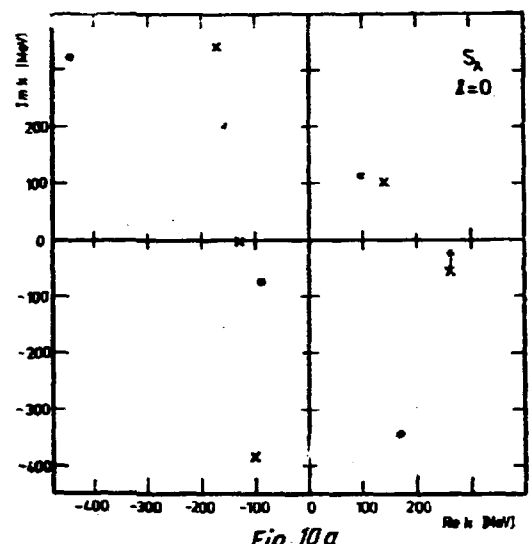


Fig. 10a

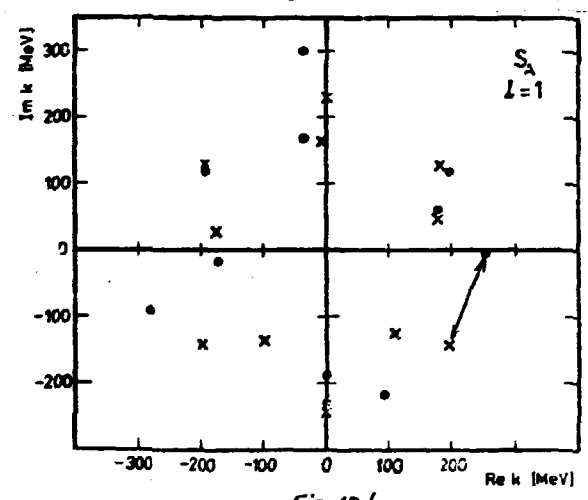


Fig. 10b

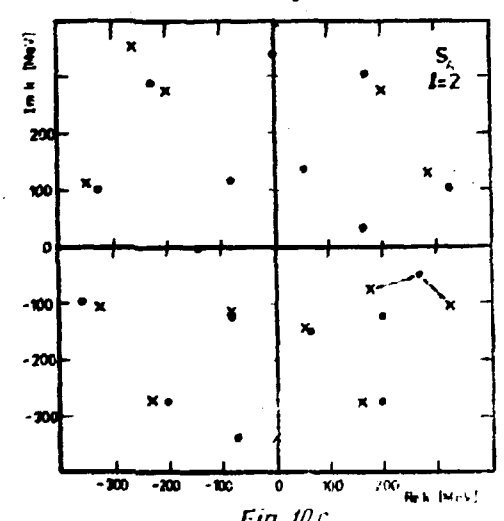


Fig. 10c

